Barite encrustation of benthic sulfur-oxidizing bacteria at a marine cold seep

E. W. N. Stevens[1], J. V. Bailey[1],*, B. E. Flood[1], D. S. Jones[1], W. P. Gilhooly III[2], S. B. Joye[3], A. Teske[4] and O. U. Mason[5]

1. Department of Earth Sciences, University of Minnesota-Twin Cities, Minneapolis, MN, USA
2. Department of Earth Sciences, Indiana University-Purdue University Indianapolis, Indianapolis, IN, USA
3. Department of Marine Sciences, University of Georgia, Athens, GA, USA
4. Department of Marine Sciences, University of North Carolina at Chapel Hill, Chapel Hill, NC, USA
5. Earth, Ocean, and Atmospheric Science, Florida State University, Tallahassee, FL, USA

*Corresponding author: J. V. Bailey. Tel.: 612 624 1603; fax: 612 625 3819; e-mail: baileyj@umn.edu

This is the author's manuscript of the article published in final edited form as:

Stevens, E. W. N., Bailey, J. V., Flood, B. E., Jones, D. S., Gilhooly, W. P., Joye, S. B., … Mason, O. U. (2015). Barite encrustation of benthic sulfur-oxidizing bacteria at a marine cold seep. Geobiology, 13(6), 588–603. http://doi.org/10.1111/gbi.12154

Barite encrustation of benthic sulfur-oxidizing bacteria at a marine cold seep

ABSTRACT

Crusts and chimneys composed of authigenic barite are found at methane seeps and hydrothermal vents that expel fluids rich in barium. Microbial processes have not previously been associated with barite precipitation in marine cold seep settings. Here we report on the precipitation of barite on filaments of sulfide-oxidizing bacteria at a brine seep in the Gulf of Mexico. Barite-mineralized bacterial filaments in the interiors of authigenic barite crusts resemble filamentous sulfide-oxidizing bacteria of the genus Beggiatoa. Clone library and iTag amplicon sequencing of the 16S rRNA gene show that the barite crusts that host these filaments also preserve DNA of Candidatus Maribeggiatoa, as well as sulfate-reducing bacteria. Isotopic analyses show that the sulfur and oxygen isotope compositions of barite have lower $\delta^{34}S$ and $\delta^{18}O$ values than many other marine barite crusts, which is consistent with barite precipitation in an environment in which sulfide oxidation was occurring. Laboratory experiments employing isolates of sulfide-oxidizing bacteria from Gulf of Mexico seep sediments showed that under low sulfate conditions, such as those encountered in brine fluids, sulfate generated by sulfide-oxidizing bacteria fosters rapid barite precipitation localized on cell biomass, leading to the encrustation of bacteria in a manner reminiscent of our observations of barite-mineralized Beggiatoa in the Gulf of Mexico. The precipitation of barite directly on filaments of sulfide-oxidizing bacteria, and not on other benthic substrates, suggests that sulfide oxidation plays a role in barite formation at certain marine brine seeps where sulfide is oxidized to sulfate in contact with barium-rich fluids, either prior to, or during,

the mixing of those fluids with sulfate-containing seawater in the vicinity of the sediment/water interface. As with many other geochemical interfaces that foster mineral precipitation, both biological and abiological processes likely contribute to the precipitation of barite at marine brine seeps such as the one studied here.

INTRODUCTION

The mineral barite ($BaSO_4$) is found in diverse depositional environments and is associated with a variety of different geologic processes and pressure-temperature conditions (e.g., Goldberg et al., 1969; Griffith & Paytan, 2012; Eickmann et al., 2014). Natural waters are typically undersaturated with respect to barite (Chow & Goldberg, 1960; Church & Wolgemuth, 1972; Monnin et al., 1999; Griffith & Rushdi et al., 2000; Paytan, 2012), and authigenic barite precipitation occurs when fluids enriched in barium (Ba^{2+}) encounter those containing sulfate (SO_4^{-2}) (Ritger et al., 1987; Torres et al., 1996; Greinert et al., 2002; Aloisi et al., 2004), according to Equation 1.

$Ba^{2+} + SO_4^{2-} <=> BaSO_4$ Equation (1)

The precipitation of authigenic barite occurs in a variety of depositional settings, including springs, hydrothermal vents and cold seeps (Aquilina et al., 1997; Arenas et al., 2000; Greinert et al., 2002; Torres et al., 2003; Eickmann et al., 2014). In marine systems, precipitation occurs at the seafloor and within the sediment column (Torres et al., 1996; Aquilina et al., 1997; Hanor, 2000; Greinert et al., 2002; Aloisi et al., 2004; Riedinger et al., 2006; Feng & Roberts, 2011; Griffith & Paytan, 2012). Diffuse precipitates also form in the water column in association with decaying organic matter

(Bertram & James, 1997; Stroobants et al., 1991; Dymond et al., 1992; Dehairs et al., 1991; Dehairs et al., 1980; Gonzalez-Muñoz et al., 2012; Goldberg & Arrhenius, 1958; Bishop, 1988). As an authigenic mineral that reflects the environment of precipitation, barite from diverse depositional environments provides robust paleoenvironmental indicators. For example, geochemical analysis of sedimentary barite offers insight regarding past patterns of marine primary productivity (e.g., Bishop, 1988; Dehairs et al., 1991; Dymond et al., 1992; Gingele & Dahmke, 1994; Paytan et al., 1996); seawater strontium (e.g., Paytan et al., 1993); redox zone migration (Contreras et al., 2013); and the sulfur isotope composition of marine sulfate from the Cenozoic (e.g., Paytan et al., 1998) to the Archean (e.g., Shen et al., 2001).

Although barite is thought to form primarily through the abiotic mixing of barium and sulfate-enriched fluids (Hanor, 2000), a number of studies suggest that, under certain conditions, microbial processes play a role in the precipitation of barite (e.g., Bertram & James, 1997; Rasmussen, 2000; Gonzalez-Munoz, 2003; Senko et al., 2004; Bonny & Jones, 2007a; Bonny & Jones, 2007b; Bonny & Jones, 2008b; Sanz-Montero et al., 2009; Gonzalez-Muñoz et al., 2012; Griffith & Paytan, 2012). Specific mechanism(s) by which microorganisms mediate barite precipitation vary and are incompletely understood. Potential mechanisms include passive or active biological enrichment of barium (e.g., Goldberg & Arrhenius, 1958; Bishop, 1988b; Ganeshram et al., 2003; Bonny & Jones, 2008b), the generation of sulfate via sulfide-oxidation (Spirakis, 1991; Senko et al., 2004; Bonny & Jones, 2008a), and cellular surfaces acting as nucleation sites for crystal precipitation (e.g., Gonzalez-Munoz, 2003; Gonzalez-Muñoz et al., 2012).

Sulfate produced during lithotrophic sulfide oxidation is generally only thought to contribute to barite precipitation in sulfate-depleted settings such as terrestrial springs (Bonny & Jones, 2008a). Sulfide oxidation in the marine environment has not previously been associated with barite precipitation because of the ubiquity of dissolved sulfate (28 mM) in seawater. In contrast to those of terrestrial springs, marine authigenic barites have, in fact, been noted for their paucity of "biological textures" (Bonny & Jones, 2008b). The canonical view is that barite precipitating at marine cold seeps is driven exclusively by the abiotic mixing of barium-rich, sulfate-free fluids with seawater rich in sulfate (Fu et al., 1994; Torres et. al. 1996; Aquilina et al., 1997; Castellini et al., 2006; Roberts et al., 2010). However, the relative contribution of sulfate produced during sulfide oxidation may become significant in certain marine pore waters where microbial sulfate reduction consumes dissolved sulfate and barite is remobilized by reductive dissolution (Fritz et al., 1989; Greinert et al., 2002; Torres et al., 2003), or where the active precipitation of authigenic barite can temporarily deplete local sulfate supply (Feng & Roberts, 2011). Additionally, some subsurface fluids, including those that are enriched in barium, lack sulfate (Joye et al., 2009). In sulfate-free marine settings such as these, lithotrophic sulfide oxidation could drive precipitation of authigenic barite, though specific evidence for this process has not, to our knowledge, been presented.

The seepage of hypersaline fluids from subsurface reservoirs can lead to the formation of pools containing high-density fluids on the seafloor. Brine pools are known from the Red Sea, the Black Sea, the Mediterranean and the Gulf of Mexico (Addy & Behrens, 1980; Eder et al., 1999; van der Wielen et al., 2005; Daffonchio et al., 2006). Brine fluids are rich in dissolved organic carbon that may stimulate dissimilatory sulfate

reduction, generating sulfide that supports the growth of sulfide-oxidizing bacteria and sustains the establishment of animal communities that depend on chemoautotrophic microbial symbionts (MacDonald et al., 1990; Greinert et al., 2002; Orcutt et al., 2005). Certain brine seepage and mud volcano sites in the Gulf of Mexico also hosts extensive authigenic barite deposits that occur where barium-rich, sulfate-free brine fluids encounter seawater sulfate (Fu et al., 1994; Castellini et al., 2006; Roberts et al., 2010). During exploration of one of these brine pools in the Gulf of Mexico, we discovered barite crusts that contain dense networks of barite-mineralized filaments internally. The mineral filaments resemble *Beggiotoa,* a filamentous sulfide-oxidizing bacterium that is extremely abundant in the microbial mats at this site. Putative *Beggiatoa*-like microorganisms have been shown previously to be preserved as fossils in ancient phosphorites and methane seep carbonates (Cavagna et al., 1999; Peckmann et al., 2004; Barbieri & Cavalazzi, 2005; Bojanowski, 2007; Bailey et al., 2013), but have not been identified previously in barite. Here we report on the results of imaging, mineralogical characterization, and sequencing of relict DNA recovered from within the barite-mineralized filaments. We complemented these analyses with laboratory experiments and isotopic analyses to further resolve the role of bacterial sulfide oxidation in the precipitation of the filament-hosting barite mineral crusts.

MATERIALS AND METHODS

Sample Localities

Green Canyon Block 246 (GC246) is located on the upper mid-continental slope of the Gulf of Mexico, approximately 200 km southwest of the Mississippi River Delta. This

region has a complex geology influenced by extensive sedimentation, sea-level changes and salt tectonics that create geochemical conditions, conduits, and topography that allow for the formation of mud volcanoes and brine seepage features (Joye, 2005; Roberts et al., 2010). Dead Crab Lake is a shallow brine pool approximately 15 m wide and 15-20 cm deep, located at a water depth of 867 m (27º42.1985'N, 90º39.0112'W). Barite crusts and chimneys, as well as extensive orange and white-colored microbial mats that were visually dominated by dense *Beggiatoa* filaments, were encountered along the shoreline of Dead Crab Lake (Fig. 1A). Samples of the mineral crust and chimney structures were collected using the DSV *Alvin* during dives 4651, 4652 & 4656 (November, 2010) on a research cruise on the R/V *Atlantis* (Cruise AT 18-02).

Observations and Sample Characterization

Initial observations and images of the barite mineral crusts and chimney samples were made using an Olympus SZX16 stereomicroscope on board the R/V *Atlantis* immediately after sample collection. Samples were split for microscopy and molecular biology using sterilized tools, with the latter sample splits being frozen immediately at -80°C. Mineral crust samples were later imaged using a Hitachi T-1000 SEM scanning electron microscope operating at an acceleration voltage of 15 kV. Semi-quantitative element abundances were measured using energy-dispersive x-ray spectroscopy (EDS) running Bruker's Quantax 50 software, with acquisition times of 90 seconds for EDS spectra. Bulk mineralogical analysis of the dried mineral crust was performed using a Rigaku Miniflex powder X-ray diffraction (XRD). The x-ray source was a Cu anode operated at 30 kV and 15 mA using CuKα radiation. Scans were taken at 2º per minute and covered

an angular region of $15^{o} \leq 2\theta \leq 65^{o}$. Mineral spectra were identified using the XRD analysis software JADE (Materials Data Incorporated, USA).

DNA Recovery from Barite Filaments and 16S rRNA Gene Analysis

Sample preparation and DNA extraction

In order to obtain mineral-hosted DNA that was free of contamination on external surfaces, barite crust samples containing mineralized filaments were washed prior to sample homogenization and DNA extraction. Washing followed a procedure similar to that used by Mason et al. (2015). For each wash step, samples were rinsed in syringe-filtered 1x phosphate buffered saline (PBS), followed by sonication at 160 watts for 15 seconds. Samples were then centrifuged for 5 minutes at 4000 × g. Supernatant was removed and fresh PBS added for a total of nine rinses. The third, sixth and ninth rinsate was collected and tested for the presence of amplifiable DNA via PCR using bacterial-specific primers 27F and 1492R and the *Beggiatoa*-specific primer pair 341F and VSOXBr (See primer details in Table S2).

After 9 wash steps, no amplifiable DNA was detected in the rinsate. Following homogenization, DNA was then extracted from the barite crust (one 0.6 g sample) using the Powersoil DNA Isolation Kit (Mo Bio Laboratories, USA) following the manufacturer's protocol, with two modifications. First, prior to bead beating, samples were incubated at 65°C for 5 minutes, vortexed briefly, and returned to 65°C for 5 minutes. Second, bead beating was performed for 5, 8 and 10 minutes, followed by the pooling of supernatants, in order to reduce extraction biases based on cell type.

iTag amplicon sequencing, data processing and analysis

An Illumina tag (iTag) amplicon library of the V3 hypervariable region of the 16S rRNA gene was generated using an approach similar to that of Bartram et al. (2011). The V3 region was amplified via polymerase chain reaction (PCR) using the Illumina-specific adaptor-primers of Bartram et al. (2011) modified to include a degenerate sequence of 4-7 nucleotides (e.g., NNNN) between the adapter sequences and the primers to improve cluster identification during Illumina sequencing. PCR reactions were performed using the HotStarTaq Plus enzyme (Qiagen, USA), with 5 minute initial denaturation at 95 ºC, 25 cycles of denaturation (95 ºC, 1 minute), annealing (50 ºC, 1 minute), and elongation (72 ºC, 1 minute), and 7 minute final elongation (72 ºC). Gel electrophoresis was used to separate DNA products from primers and primer dimers using a 2% agarose gel. Bands were cut out and purified using the Zymoclean Gel DNA Recovery Kit (Zymo Research, Orange, CA). Itag amplicon libraries were sequenced via 150 cycles of paired-end Illumina MiSeq at the University of Minnesota Genomics Center (UMGC).

Raw sequences were quality trimmed and filtered using Fastq-MCF (Aronesty, 2011) and reads with adaptor sequences removed using cutadapt (Martin, 2011). Forward and reverse sequences were assembled using PAired-eND Assembler (Masella et al., 2012). Chimeras were removed using UCHIME (Edgar et al., 2011). Sequence data was then processed using mothur (Schloss et al., 2009) within the Galaxy platform (Blankenberg et al., 2010; Giardine et al., 2005), which was used to classify sequences according to SILVA taxonomic assignments (Quast et al., 2013). Operational taxonomic units (OTUs) were defined at 97% similarity using default parameters. Rarefaction analyses of both the general 16S rRNA gene clone library and the 16S rRNA gene Illumina amplicon data sets

were also performed using mothur (Schloss et al., 2009). Amplicon sequences were deposited in the Sequence Read Archive (http://www.ncbi.nlm.nih.gov/sra) under project ID PRJNA267505.

Clone libraries

Two 16S rRNA gene clone libraries were generated. The first used the general bacterial primers 27F and 1492R (Table S2) to improve phylogenetic resolution of the dominant taxa. A second clone library was generated using the primer pair VSOXBr and 341f (Table S2) in order to target representatives of the Beggiatoaceae that are commonly missed by widely-used general primer sets (Kalanetra et al., 2005). Amplification using 341F and VSOXBr required two consecutive PCRs using the same primer sets, an approach described in Salman et al. (2011). PCR reactions (25 µl) were incubated as follows: initial denaturation of 4 minutes at 95 ºC, 6 cycles of touchdown PCR consisting of 45 seconds of denaturation at 95 ºC, annealing for 45 seconds at temperatures of 59 ºC, 57 ºC, 55 ºC, and elongation for 45 seconds at 72 ºC, followed by 24 cycles of PCR at an annealing 53 ºC for 45 seconds, with a final elongation step at 72 ºC for 7 minutes. PCR products were then cloned using the Topo TA cloning kit (Invitrogen, USA). PCR products were cleaned using a DNA Clean and Concentrator -5 kit (Zymo Research, USA. Sanger sequencing was performed at the UMGC with a capillary ABI 3730xl sequencer and ABI BigDye Terminator version 3.1 chemistry (Applied Biosystems, USA). Partial sequences were assembled using Sequencher (Bromberg et al., 1995) with final sequence lengths of >1300 bp reads for the general bacterial library and >500 bp

reads for the *Beggiatoa* specific library. Clone library sequences were archived under GenBank accession numbers KM396655-KM396693.

Phylogenetic analysis

The 16S rRNA gene sequences from the general bacterial and *Beggiatoa*-specific clone libraries were aligned using the NAST aligner within the Greengenes web application (DeSantis et al., 2006). The sequences were then added to an ARB database of nearly 480,000 representative bacterial sequences. Manual refinement was performed in ARB using the ARB_Edit4 sequence editor. Alignments were trimmed so that all sequences were of equal length, and nucleotide positions with less than 50% base-pair conservation were masked. The final alignment lengths were 1320 and 512 nucleotide positions for the general bacteria library and *Beggiatoa* specific library respectively. Neighbor joining analyses were performed in PAUP* version 4b10 (Swofford, 1999) with Jukes-Cantor (JC) corrected distance matrix and 2000 bootstrap replicates.

Precipitation Experiments

To investigate the mechanisms by which sulfide-oxidizing bacteria might induce barite precipitation via the generation of sulfate in barium-rich solutions, experiments were conducted using five pure culture isolates. Two of these isolates, namely *Thiomicrospira crunogena* strain XCL-2 (Jannasch et al. 1985; Scott 2006) (ATCC = 35932; DSMZ = 25203) and *Sedimenticola thiotaurini* strain SIP-G1 (Flood et al., 2015) (ATCC = BAA-2640; DSMZ = 28581), were selected because they are known to oxidize sulfide and thiosulfate. *S. thiotaurini* SIP-G1 was isolated from Sippewissett Salt Marsh, MA. *T.*

crunogena XCL-2 was originally isolated from hydrothermal sulfides of the East Pacific Rise (Jannasch et al., 1985). We isolated three additional strains from sediment collected in the Gulf of Mexico (Site GC233) near the site of barite crust collection. These organisms were isolated on the experimental precipitation medium agar plates described below, with the addition of thiosulfate, but without the addition of barium. These strains were taxonomically characterized by amplification and analysis of 16S rRNA genes as described for the clone libraries. The three strains are herein referred to as *Halomonas* sp., strain BM23 (KP336666), *Maribacter* sp. strain LM2 (KP336667) and *Roseobacter* sp. strain LH4 (KP336667).

PCR amplification using *sox*B specific primers, soxB693F and soxB1446B (Petri et al., 2001), was performed on all five isolates in order to assess the presence or absence of a *Sox* pathway, a pathway that diverse lithotrophs use to oxidize sulfur (Mukhopadhyaya et al., 2000; Kappler & Dahl, 2001),. PCR analysis showed that *Roseobacter sp.* LH4, *S. thiotaurini,* and *T. crunogena* were positive for *sox*B. No *sox*B gene amplification was observed for *Maribacter* and *Halomonas*. *Halomonas* sp. strain BM23 was chosen for inclusion in these experiments because previous work with related bacteria (Teske et al., 2000) suggested that its sulfur metabolism generates tetrathionate (and perhaps sulfate), but at a slower rate than the other sulfur-oxidizing strains selected here. *Maribacter* sp. strain LM2, a organoheterotroph, was chosen as a control strain because it does not likely have the capability to oxidize thiosulfate, but grows on the same plates as the other bacteria probably via the degradation of trace organics or structural proteins within the agar.

Precipitation experiments and bacterial isolations were conducted using an agar base medium with the following composition: 430 mM NaCl, 6.0 mM $MgCl_2$ $6H_20$, 2.0 mM $CaCl_2$, 3.3 mM NH_4Cl, 3.1 mM K_2HPO_4, 10 mM Tris.Cl buffer, , 0.005% phenol red (w/v), 1x SL-8 trace metal solution (Biebl and Pfennig, 1978) and 1.5% technical grade agar (w/v) (BD Difco). Plates used during precipitation experiments consisting of the base media supplemented with 2 mM $BaCl_2$ and 10 mM $Na_2S_2O_3$. Phenol red was used as a pH indicator and base media was adjusted to pH 7.92. These plates were designed to promote thiosulfate oxidation coupled with autotrophic growth whereby NH_4 and PO_4 serve as inorganic sources of N and P. Although Tris Cl provides some initial buffering capacity to promote microbial growth, sufficient levels of acid or base production around a microbial colony turns the phenol red yellow for acid production and fushia for base production. Prior to initiation of precipitation experiments, all isolates were cultured in liquid Marine Broth 2216 (BD Difco) except for *T. crunogena*, which was cultured in liquid TMS media (Jannasch et al., 1985). All cultures were incubated for 72 hours at 25º ± 1º prior to inoculation of the barite precipitation experiments.

Aliquots (20 µl) of the liquid culture inocula were spread on the experimental plates. Petri dishes were stored benchtop at 25º ± 1º. *S. thiotaurini* was grown in a Coy hypoxic chamber (5% O_2) due to its sensitivity to oxygen – a characteristic that it shares with some closely related sulfide-oxidizing gammaproteobacteria, including marine *Beggiatoa* strains. Experiments were monitored daily for cell growth, mineral precipitation, and changes in pH. Plates with 2mM $BaCl_2$ and ~10 mM $Na_2S_2O_3$, but without cell inocula, were used as cell-free control experiments. Additional controls were also performed

using cells fixed in a 4% paraformaldehyde in seawater solution incubated at 4ºC for 3 hours.

Isotopic Analysis

The sulfur ($\delta^{34}S$) and oxygen ($\delta^{18}O$) isotopic compositions of barite powders drilled from barite crusts, barite-mineralized filaments and barite chimneys, were measured on a stable isotope ratio mass spectrometer (IRMS; Thermo Delta V Plus at IUPUI). Barites were weighed (0.4 mg) into tin capsules and mixed with vanadium pentoxide to promote complete combustion to SO_2 in an elemental analyzer (Costech Analytical ECS 4010), which was coupled under continuous flow to the IRMS. A separate barite split (0.15 mg) was weighed into silver capsules and mixed with an equal mass of graphite. Sulfate-oxygen was converted to CO by pyrolysis (Thermo TC/EA) and the sample gas was transferred by helium carrier gas to the IRMS for oxygen isotope analysis. Isotope values were reported in standard delta notation [$\delta^{x}E = (R_{sample}/R_{standard} - 1) \times 1000$] for each isotope ($^{x}E = {}^{34}S$ or ^{18}O) by normalizing the isotopic ratio ($R = {}^{34}S/{}^{32}S$ or $^{18}O/^{16}O$) of the sample to the isotopic ratio of the international standard for sulfur, Vienna Canyon Diablo Troilite (VCDT), and Standard Mean Ocean Water (SMOW) for oxygen. Sulfur isotope values were calibrated against international reference materials NBS-127 ($\delta^{34}S$ = 21.1‰), IAEA-SO5 ($\delta^{34}S$ = 0.49‰), and IAEA-SO6 ($\delta^{34}S$ = -34.05‰). Oxygen isotope values were normalized to reference materials IAEA-SO6 ($\delta^{18}O$ = -11.0‰), NBS-127 ($\delta^{18}O$ = 8.7‰), and IAEA-SO5 ($\delta^{18}O$ = 12.0‰). Linear regression was used to correct unknowns to the international reference values and to account for scale compression. Analytical precision for $\delta^{34}S$ and $\delta^{18}O$ values of reference materials was ±0.2‰ (1σ).

RESULTS

Observations and mineralogical characterization of mineral filaments

A complex assemblage of mineral crusts, chimneys, brine flow channels, and microbial mats containing abundant *Beggiatoa* surround the Dead Crab Lake brine pool (Fig. 1A). Fist-sized samples of mineral crust and small cone-shaped chimney structures were collected using the DSV *Alvin* (Table S2). As with other barite crusts and chimneys from the Gulf of Mexico, the samples collected were relatively porous and friable. Examination of the freshly collected crust using a dissecting microscope revealed a dense network of mineral filaments in the interiors of several barite crust samples (Fig. 1B). Living unmineralized filamentous sulfur bacteria resembling *Beggiatoa* were observed on crust exteriors, but in much lower abundance than in the microbial mats from the sediments in the vicinity of the crusts. Examination of the crusts using scanning electron microscopy revealed fully mineralized filaments and some organic bacterial filaments that were partially coated or encrusted by barite (Fig. 1C-D). As these filaments accumulate precipitates, they appear to grow thicker (sometimes substantially thicker than the original cell) and the filamentous morphology grades into an amorphous mineral texture (Fig. 1, Fig. S1). XRD analysis revealed that the mineral crusts and filament-encrusting minerals are composed principally of barite (Fig. S2).

Analysis of mineral-hosted DNA

DNA was extracted from the barite to determine whether the mineralized filaments preserved molecular signatures of *Beggiatoa* or other sulfide-oxidizing bacteria that may

have influenced barite precipitation. iTag amplicon sequencing of the 16S rRNA gene provided a broad picture of the community DNA preserved within the mineral matrix of the filament-hosting barite crust, while clone libraries were used to obtain greater phylogenetic resolution of certain abundant taxa.

The Illumina MiSeq iTag amplicon library produced 102,664 sequences for the single filament-hosting barite crust sample. The most abundant sequences fell within the Proteobacteria, with gammaproteobacterial sequences comprising 37.7% of the sequences and alphaproteobacterial sequences comprising 16.2% (Figure 2). Of the gammaproteobacterial sequences, 20% fell within the Thiotrichales [1], including 38 sequences from within the family Beggiatoaceae. Of the alphaproteobacterial sequences, *Roseobacter* was the most abundant genus, comprising 38% of the sequences. The most abundant sequences within the Epsilonproteobacteria fell within the genera *Sulfurovum*, *Sulfuricurvum*, *Sulfurospirillum*, and *Sulfurimonas* comprising 58%, 18%, 16%, and 4.6% of the epsilonproteobacterial sequences respectively. Molecular signatures of sulfate-reducing bacteria were also present within the crust. Of the deltaproteobacterial sequences 32%, 26%, and 5% were of the order Desulfobacterales, Desulfuromonadales, and Desulfovibrionales respectively.

Thirty-eight nearly full-length 16S rRNA gene sequences were generated from the bacterial clone library of the same sample used to generate the amplicon library, here using the primer set 27F and 1492R (Table S2). A neighbor-joining tree shows

[1] The “Thiotricales” is a polyphyletic assemblage of mutually distinct families including the Beggiatoaceae (Salman et al., 2011). Here we refer to the Thiotricales for the purposes of maintaining consistency with the current Silva taxonomy that is used for phylogenetic assignment of iTag sequences in this report.

phylogenetic relationships of the sequences from the general bacterial 16S rRNA gene clone library (Fig. 3). Numerous sequences in the clone library record the presence of sulfide-oxidizing bacteria in the depositional environment from which the barite crusts precipitated (Highlighted in Figure 3). Seven sequences fell within the Alphaproteobacteria and grouped with the family *Rhodobacteraceae*, which include the known sulfide-oxidizing bacteria genera *Roseobacter, Sulfitobacter,* and *Roseovarius* (Buchan et al., 2005). Four sequences fell within the Epsilonproteobacteria, two of which grouped with *Sulfurospirillum* and two of which grouped with *Sulfurovum*, both known sulfide-oxidizing bacteria (Campbell et al., 2006). Other phylotypes in the clone library fell within the Bacteroidetes, Firmicutes, and unclassified bacteria. The clade-specific clone library targeting the Beggiatoaceae, again from the same barite sample, used primers 341F and VSOXbR (Salman et al., 2011) (Figure 2), and produced nine sequences, two of which clustered with *Candidatus* Maribeggiatoa vulgaris (Fig. 3, green-labels).

Precipitation Experiments

Laboratory cultures of four sulfur-oxidizing bacteria and one organoheterotrophic control organism were incubated on barium-rich media to observe the influence of sulfate generation via sulfur oxidation under barium-rich, sulfate-poor conditions. Such conditions are encountered in brine pool settings like that of Dead Crab Lake where mineralized *Beggiatoa* filaments were discovered. *Beggiatoa spp.* were not selected as test strains because a marine *Beggiatoa* culture was not available and because *Beggiatoa* enrichments require gradient media and other geochemical conditions that make them impractical for these mineral precipitation experiments. Thiosulfate was used instead of

sulfide because it is easier to manipulate in laboratory experiments. Thiosulfate is readily oxidized by diverse lithotrophs that also oxidize hydrogen sulfide, and its oxidation also yields sulfate and protons, the chemical species thought relevant to barite precipitation:

$$S_2O_3^{2-} + H_2O + 2\ O_2 \rightarrow 2\ SO_4^{2-} + 2H^+ \qquad \text{Equation 4}$$

Development of observable barite precipitates varied between the five experimental isolates. Barite precipitation was observed in *Roseobacter* sp. colonies on the third day of the experiment (Figure 1F, Figure S4). *Thiomicrospira crunogena* showed barite precipitation by the fourth day of the experiment. *S. thiotaurini* colonies exhibited barite precipitates on the tenth day after inoculation. *Halomonas* sp. exhibited no barite or other mineral precipitation until 45 days after inoculation. Density, concentration, and location of the precipitates associated with *Halomonas* sp. were similar to those exhibited by the other sulfur-oxidizing bacteria. Barite precipitates developed by the twelfth day on plates with the heterotrophic control isolate, *Maribacter* sp.; although unlike with the other isolates where minerals precipitated directly and exclusively on the colony biomass, *Maribacter*-associated precipitates were always restricted to a circular halo ~5 mm away from the colony (Figure S4). Barite precipitates were not observed to form on colony biomass with *Maribacter*, in direct contrast to the sulfide-oxidizing bacterial isolates tested. Mineral precipitates on colonies (or in the region surrounding the colonies in the case of *Maribacter* sp.) were characterized using an XRD microdiffractometer. XRD analysis of all five bacterial isolates show peaks that closely resemble reference peaks for barite (Fig. S3). Uninoculated control plates showed no mineral-precipitation or XRD signal. PFA-fixed cells were also examined and no mineral precipitation was observed with the PFA-fixed controls.

Changes in pH, as reflected in a color change of the phenol red within the agar, occurred before mineral precipitation was easily observed by eye on the agar plates. In the case of *T. crunogena*, *Roseobacter* sp. and *S. thiotaurini* the agar around the cell colonies turned yellow from acid production. Initial growth of the halomonad, on the other hand, resulted in a darkening or more fuchsia appearance of the agar plate suggestive of tetrathionate production. But after 45 days the agar plates returned to their original color and barite crystals were observed. Lastly, growth of *Maribacter* sp. turned the agar plate slightly more yellow but the pH change occurred more diffusely throughout the agar plate and was not localized around the bacterial colonies.

Sulfur and oxygen isotopes of barites

Sulfur and oxygen isotopic compositions of barite mineralized filaments, barite crusts, and subsamples of barite chimneys are provided in Table S1 and plotted in Figure 4. The barite samples studied here show little variability between samples, with $\delta^{34}S$ values that ranged from 21.2 to 21.9‰, and $\delta^{18}O$ that ranged from 9.6 to 10.4‰. Although slightly enriched in ^{34}S and ^{18}O relative to Gulf of Mexico bottom water sulfate [$\delta^{34}S$ = 20.3‰, and $\delta^{18}O$ = 9.7‰ (Aharon & Fu, 2000)], GC246 barites have lower $\delta^{34}S$ and $\delta^{18}O$ values in comparison to other barite samples from the Gulf of Mexico reported by (Feng & Roberts, 2011) (Fig. 4).

DISCUSSION

Barite mineral filaments are encrusted *Beggiatoa*

411 The sediments on the shoreline of Dead Crab Lake were covered with microbial mats
412 predominated by filamentous sulfide-oxidizing *Beggiatoa* sp. [2] (Fig. 1A). The barite-
413 mineralized filaments preserved in crust samples from two sites at GC246 at the margins
414 of these mats are of similar size and morphology to *Beggiatoa*, and sometimes exhibit
415 apparent septations that resemble the linear arrangement of cells within the trichomes of
416 *Beggiatoa*, (Fig. 1C). Additionally, the observation of unmineralized and partially
417 mineralized *Beggiatoa* (Fig. 1D, E), in and on the same samples that contain the barite
418 mineral filaments suggests a continuum in the encrustation of *Beggiatoa*, from
419 completely mineral-free, to partially mineralized, to fully mineral-encrusted filaments
420 that become a structural component of the barite crust. Our conclusion that the mineral
421 filaments are encrusted *Beggiatoa* is further supported by the recovery of 16S rRNA
422 genes closely related to *Candidatus* Maribeggiatoa vulgaris in the clone libraries that
423 were produced from samples that contain mineralized filaments (Fig. 3). While it is
424 possible that living cells were present in void spaces within the crust, the lack of
425 amplifiable DNA in rinsate fluids tested prior to DNA extraction from the crust, as well
426 as the presence of partially mineralized *Beggiatoa* filaments in portions of the crust,
427 suggest that at least some of the *Beggiatoa* DNA is coeval with barite precipitation. It is
428 not surprising that *Maribeggiatoa* 16S rRNA gene sequences represent a relatively minor
429 portion of the libraries here, given that numerous other studies have reported difficulties
430 with amplifying 16S rRNA gene sequences from samples visibly dominated by

[2] We use "*Beggiatoa*" here to refer to the polyphyletic group of non-sheath-forming filamentous sulfide-oxidizing bacteria within the family Beggiatoacaea. Sequence data suggest that at least some of the organisms in the "*Beggiatoa*" mats are representatives of the candidate genus Ca. *Maribeggiatoa (Salman et al., 2011).*

Beggiatoa and related organisms in the family Beggiatoaceae (e.g., Sekar 2006; Salman et al., 2012; Jones et al., 2015).

In the barite crust samples studied here, bacterial filaments are the only identifiable organic surfaces covered with barite crystals and void space was observed between some neighboring filaments (Fig. 1B). Regions containing dense accumulations of obvious mineral filaments are commonly surrounded by massive barite crusts that gradationally exhibit less filamentous textures (Fig. S1). Dense networks of mineral filaments can take on a clotted appearance similar to the more massive barite crystal aggregates that make up the bulk of the crust exterior (Fig. S1). These microfacies relationships suggest that, at least in the samples we examined, precipitation was initiated on the filaments and these initial precipitates served as a foundation for the precipitation of a more massive authigenic crust. Fig. 1C-D shows barite crystallites precipitating preferentially on *Beggiatoa* filaments. Whether mineralized filaments are foundational to the extensive authigenic barite crusts present at this site, or other brine seeps, remains an open question. However, samples containing mineralized filaments were collected on two separate submersible dives in three different samples collected at GC246, so they are clearly common at this site. Other benthic substrates such as rocks, sediment grains, and mussel shells, were not encrusted by barite at this site.

In addition to hosting the molecular remains of *Candidatus* Maribeggiatoa, the filament-hosting crusts from the Gulf of Mexico also contain genetic material from other bacteria, including other known sulfide-oxidizing bacteria (Figs. 2-3). Broad phylogenetic trends observed in the 16S rRNA gene iTag amplicon library of mineral-hosted DNA were very similar to those obtained in the bacterial clone library (Fig. 2). Both the clone library and

454 the iTag amplicon dataset showed that diverse sulfide-oxidizing bacteria were present in
455 the microenvironment from which the barite precipitated. The recovery of sequences
456 representing taxa within the orders Desulfobacterales, Desulfuromonadales, and
457 Desulfovibrionales (Figure 2) further suggest that sulfate reduction may have been
458 occurring in close spatial proximity to sulfide oxidation, and that a community actively
459 involved in sulfur cycling was entombed by barite precipitation.
460
461 **Is barite encrustation of cells induced by sulfide-oxidation?**
462 The generation of sulfate by sulfide-oxidizing bacteria is thought to promote barite
463 precipitation in certain modern non-marine settings where sulfate is absent or found only
464 in low concentrations (Senko et al., 2004; Bonny & Jones, 2008a). Bacterial sulfide-
465 oxidation has also been invoked to explain the patchy occurrence of authigenic barite in
466 Miocene lake deposits (Sanz-Montero et al., 2009). In the marine environment where
467 sulfate is abundant, bacterial sulfide oxidation is not considered relevant to barite
468 precipitation. However, certain brine fluids, such as those at Dead Crab Lake, are
469 enriched in barium and free of measurable sulfate, raising the possibility that sulfate
470 production via lithotrophic sulfide oxidation leads to barite precipitation.
471 We exposed laboratory cultures of sulfide-oxidizing bacteria and organoheterotrophic
472 control organisms to barium-rich culture conditions to determine whether sulfide-
473 oxidation would promote rapid cell barite encrustation of cell material, reminiscent of
474 what is observed in the barite-encrusted *Beggiatoa* from the Gulf of Mexico. Barite
475 precipitated on *Roseobacter* sp. colonies within three days of inoculation, and on *T.*
476 *crunogena* colonies after four days. Barite precipitated on other sulfide-oxidizing strains

as well, but precipitate formation was slower than with *Roseobacter sp.* or *T. crunogena*. The observation that barite precipitation occurred most rapidly on *Roseobacter* and *T. crunogena* colonies may be explained by the fact that both of these organisms possess a complete *Sox* sulfur oxidation pathway, including those genes that code for the SoxCD subunits (Scott et al., 2006). These organisms oxidize thiosulfate directly to sulfuric acid without producing elemental sulfur intermediates (Meyer et al., 2007).

Like *Beggiatoa, S. thiotaurini* has an incomplete *Sox* sulfide oxidation pathway, which results in the production of elemental sulfur. Sulfur bacteria with incomplete *Sox* pathways, such as *Beggiatoa* and *S. thiotaurini*, require other pathways, such as the pathway that uses reverse dissimilatory sulfate reductase (rDsr), in addition to a partial *Sox* pathway, to oxidize elemental sulfur to sulfite and ultimately sulfate (Mußmann et al., 2003). Because *S. thiotaurini* produces elemental sulfur intermediates before it produces sulfate, we might predict that sulfate production, and concomitant barite precipitation, would be slower with *S. thiotaurini*, and indeed barite precipitation did not occur until the tenth day of the experiment with strain *S. thiotaurini*.

In *Halomonas* sp., tetrathionate, rather than sulfate, is the primary end product of thiosulfate oxidation (Sorokin et al., 1999; Podgorsek & Imhoff, 1999). *Halomonas* sp. colonies did not exhibit barite precipitation until 45 days after inoculation. PFA-fixed control cells did not exhibit barite precipitates in any of these strains, suggesting that thiosulfate oxidation in these experiment was responsible for sulfate production and barite precipitation. Precipitates were found in association with the organoheterotroph *Maribacter* sp., but instead of the barite precipitating on colony biomass, as it had with the sulfide-oxidizing strains, barites associated with *Maribacter* sp. occurred only as

halos that formed >5 mm away from the colony biomass. Mineral precipitates were never observed on *Maribacter* colony biomass. Similar halo production has previously been reported in several *Vibrio* species grown on sulfate-containing agar medium and is thought to result from sulfatase activity (Kitaura et al., 1983). Additionally agar-degrading bacteria have the potential to form pits in agar-based media. Members of the Bacteroidetes, especially members of the Flavobacteria, are known to degrade agar. These organisms can potentially hydrolyze carrageenan, which is a sulfated polysaccharide found in the red algae from which the agar is derived (Michel et al., 2006). If carrageenans in the agar were hydrolyzed by *Maribacter*, bound sulfate would be released, which could explain the halo-shaped barite precipitates observed in the organoheterotroph control experiments. But importantly, barite did not precipitate on the cell biomass as it did with all tested cultures of sulfide-oxidizing bacteria. Our interpretations of microbial physiology as it relates to barite precipitation are supported by our observations of pH changes reflected in the color change of phenol red.

The results of the precipitation experiments demonstrate that under sulfate-depleted conditions, the oxidation of reduced sulfur compounds such as hydrogen sulfide and thiosulfate can result in the rapid precipitation of barite that is localized on cell biomass. In some cases, barite precipitation was rapid enough to entomb cells (Fig. 1G). The brine fluids from Dead Crab Lake are enriched with barium, but lack sulfate (Joye et al., In Preparation). Feng and Roberts (2011) also note that the precipitation of barite can locally deplete sulfate, creating a zone of depletion that may provide opportunities for sulfide oxidation to contribute sulfate to barite formation. At Dead Crab Lake, extensive mats of *Beggiatoa* occupy the interface between seawater and brine fluids. Our experimental

results suggest that if brine fluids encountered sulfide diffusing from microbial sulfate reduction in subjacent sediments, then the production of sulfate from sulfide-oxidation has the potential to trigger rapid barite precipitation and encrustation of *Beggiatoa* biomass as recorded by the barite-mineralized filaments. Additionally, the precipitation of extensive barite precipitates on non-filamentous bacteria in our precipitation experiments, and the recovery of DNA from non-filamentous sulfur bacteria from the barite crusts, leaves open the possibility that amorphous barite precipitates formed on non-filamentous bacteria, but unlike the mineralized filaments, there is no specific morphological evidence that this occurred.

Did sulfur oxidation play a role in the formation of Gulf of Mexico barite crusts?

Paired $\delta^{34}S$ and $\delta^{18}O$ analysis provide a record of the source and diagenetic history of sulfate incorporated into sedimentary barites. Isotope fractionations produced during enzymatic reactions within sulfate-reducing bacteria tend to generate residual pools of ^{34}S-enriched and ^{18}O-enriched sulfate, although the isotope effects are different for sulfur and oxygen (Brunner et al., 2005; Bradley et al., 2011). The isotopic offset between sulfate and sulfide that is produced during dissimilatory sulfate reduction can be large in magnitude (up to 66‰), and tends to decrease when sulfate reduction rates are elevated (Sim et al., 2011; Leavitt et al., 2013), or when sulfate concentration is limiting (Habicht et al., 2002). In batch experiments, rate-dependent sulfur isotope fractionations appear to be largely controlled by electron donor supply (Leavitt et al., 2013), and in natural systems, higher sulfate reduction rates are associated with lower isotope fractionations as measured in oil and gas seeps of the Gulf of Mexico (Aharon and Fu, 2000). Residual

546 sulfate-oxygen isotope values also increase as a function of sulfate reduction; however,
547 the overall effect is governed by equilibrium oxygen isotope exchange between
548 intracellular sulfoxy ions and ambient water (Brunner et al., 2005; Wankel et al., 2014).
549 In addition to the pathway of dissimilatory sulfate reduction, consortia of methanotrophic
550 archaea and sulfate-reducing bacteria can couple anaerobic oxidation of methane to
551 sulfate reduction (AOM-SR) in sedimentary environments where sulfate and methane
552 gradients overlap (Boetius et al., 2000; Orphan et al., 2001; Joye et al., 2004; Orcutt et
553 al., 2005; Milucka et al., 2012). The sulfur and oxygen isotope fractionations during
554 AOM-SR are similar in magnitude to sulfate reduction and tend to decrease in methane
555 charged gas seeps (Deusner et al., 2014).
556 Regardless of the microbiota or their biochemical pathways, barites that form within the
557 zone of sulfate reduction at hydrocarbon seeps tend to record a trend of increasing $\delta^{34}S$
558 and $\delta^{18}O$ sulfate values such as those expected from microbial sulfate reduction (Aharon
559 & Fu, 2000; Feng & Roberts, 2011). The authigenic barites studied here were enriched in
560 ^{34}S and ^{18}O relative to contemporaneous seawater (Fig. 4); however, authigenic barites
561 from other methane seeps generally have comparatively higher $\delta^{34}S$ and $\delta^{18}O$ values
562 (Feng & Roberts 2011). Feng and Roberts (2011) proposed that barite crusts with higher
563 $\delta^{34}S$ and $\delta^{18}O$ values formed beneath the sediment/water interface under conditions
564 where barium fluxes are relatively low, and efficient bacterial sulfate reduction can drive
565 residual pore water fluids toward greater enrichment in ^{34}S and ^{18}O. Conversely, barites
566 that precipitate at the sediment/water interface have $\delta^{34}S$ and $\delta^{18}O$ values closer to
567 seawater values, but slightly enriched in ^{34}S and ^{18}O, similar to that observed here, a
568 correlation that has been attributed to less efficient sulfate reduction in a more open

569 system (Feng and Roberts, 2011). This interpretation explains at least some of the
570 disparity in isotope values seen in barites that formed at, or above, the sediment/water
571 interface relative to those that precipitated in the sediments.

572 In the case of the barite samples studied here, molecular evidence suggests a close
573 spatial association between sulfate-reducing bacteria and sulfide-oxidizing bacteria. We
574 suggest that one additional aspect of the more geochemically-open system near the
575 sediment/water interface is the presence of sulfide-oxidizing bacterial mats that can
576 shuttle sulfide to sulfate during sulfur oxidation. The relatively small sulfur isotope
577 effects (± 5‰) that occur during biological sulfide oxidation (Fry et al., 1986; Zerkle et
578 al., 2009; Brabec et al., 2012), would produce sulfate with low $\delta^{34}S$ values that, when
579 mixed with the local pool of dissolved sulfate in the microenvironment from which the
580 barite precipitated, can result in barite with muted ^{34}S-enrichments. Oxygen isotope
581 exchange during sulfide oxidation can also contribute to low $\delta^{18}O$ values. The oxidation
582 effects are likely buffered by co-precipitation of contemporaneous seawater sulfate in the
583 barite crusts studied here. The presence of molecular signatures indicating a close
584 association between sulfate-reducing bacteria and sulfide-oxidizing bacteria, and the
585 precipitation of barite directly on mats of sulfide-oxidizing bacteria within the barite
586 crusts, provide evidence for an active oxidative sulfur cycle. This microenvironment
587 fosters barite precipitation where sulfide oxidation potentially contributed, at least in part,
588 to the precipitation of barite on cell biomass, leading to mineral entombment of the kind
589 that is observed in samples from Dead Crab Lake brine pool. The localization of barite
590 precipitates on filaments of sulfide-oxidizing bacteria, as opposed to other benthic
591 substrates such as rocks, shells or sediment grains, also supports the idea that sulfide

592 oxidation may have played a role in the encrustation of the filaments by barite. We
593 suggest that the barite crusts observed in this study, which are slightly enriched in ^{34}S and
594 ^{18}O relative to seawater, formed at an interface in which both seawater sulfate and
595 sulfide-oxidation supplied sulfate for the precipitation of barite.
596
597 **CONCLUSIONS**
598 Chemolithotrophic microbes commonly colonize interfaces between geochemical
599 zones, such as the gradients conditions between reduced sulfur and oxygen, or reduced
600 iron and oxygen. At these geochemical interfaces, abiotic oxidation reactions that are
601 thermodynamic favorability may be kinetically slow (Gartman et al., 2011). The
602 metabolic activity of lithotrophic organisms, along with the potential of cells to serve as
603 nucleation sites, can increase the rate of precipitation of minerals at such interfaces, and
604 influence the physical and chemical characteristics of any precipitates that may form.
605 Mats of sulfide-oxidizing bacteria colonize steep geochemical interfaces separating
606 anoxic, sulfidic, barium-rich fluids, and oxic, sulfate-rich bottom waters, at brine pools in
607 the Gulf of Mexico. These sediments are provided with hydrogen sulfide produced by
608 dissimilatory sulfate reduction in surrounding sediments. If microbes were not present at
609 this interface, barite would (and does) precipitate as barium-rich fluids encounter
610 seawater that contains sulfate (Fu et al., 1994; Torres et. al. 1996; Aquilina et al., 1997;
611 Castellini et al., 2006; Roberts et al., 2010). However, mats of sulfide-oxidizing bacteria
612 can also generate sulfate through the oxidation of sulfide and/or provide substrates for
613 mineral nucleation in this zone. The mineralized filaments described here precipitated
614 under conditions that were not directly observed, and the isotopic composition of the

barite-encrusted filaments do not, by themselves, provide unambiguous evidence of sulfide oxidation contributing to barite precipitation. However, the isotopic values are fully consistent with a depositional environment in which sulfide oxidation is occurring and contributing sulfate to barite precipitation. Laboratory experiments show that sulfate evolved from sulfide oxidation in simulated brine fluids leads to rapid barite precipitation on cell biomass, encrusting sulfide-oxidizing bacteria in a manner reminiscent of the encrustation on *Beggiatoa* observed in the Gulf of Mexico barite crusts studied here. Our observations suggest that bacterial sulfide oxidation may be involved in barite precipitation under certain marine conditions, via the production of sulfate in a manner similar to that already known to occur in non-marine environments (e.g., Senko et al., 2004; Bonny & Jones, 2008a). The expansion of the environments in which bacterial sulfide oxidation is suspected to facilitate barite precipitation introduces new possibilities for the origins of certain ancient barite deposits. Additionally, the discovery of barite mineralization of *Beggiatoa* in modern marine sediments extends the fossilization potential of these organisms beyond their currently known preservation in carbonates and phosphorites, and opens up the possibility that they are preserved in ancient marine barite deposits as well.

ACKNOWLEDGEMENTS

We thank the crew, SSG, and science team of research cruise AT18-2 (upon which these samples were collected) onboard the R/V *Atlantis* with the HOV *Alvin*, funded by the National Science Foundation (EF-0801741 to SBJ). Portions of this work were supported

by a National Science Foundation grant EAR-1057119 to JVB. Cassandra Ho, who was funded by a Howard Hughes Medical Institute internship, isolated the Gulf of Mexico strains used in the mineral precipitation experiments. Elizabeth Ricci performed PCRs that allowed for strain identification. This work was carried out in part using resources at the University of Minnesota Characterization Facility, which receives partial support from NSF through the MRSEC program, the University of Minnesota Supercomputing Institute, and University of Minnesota Genomics Center.

FIGURES

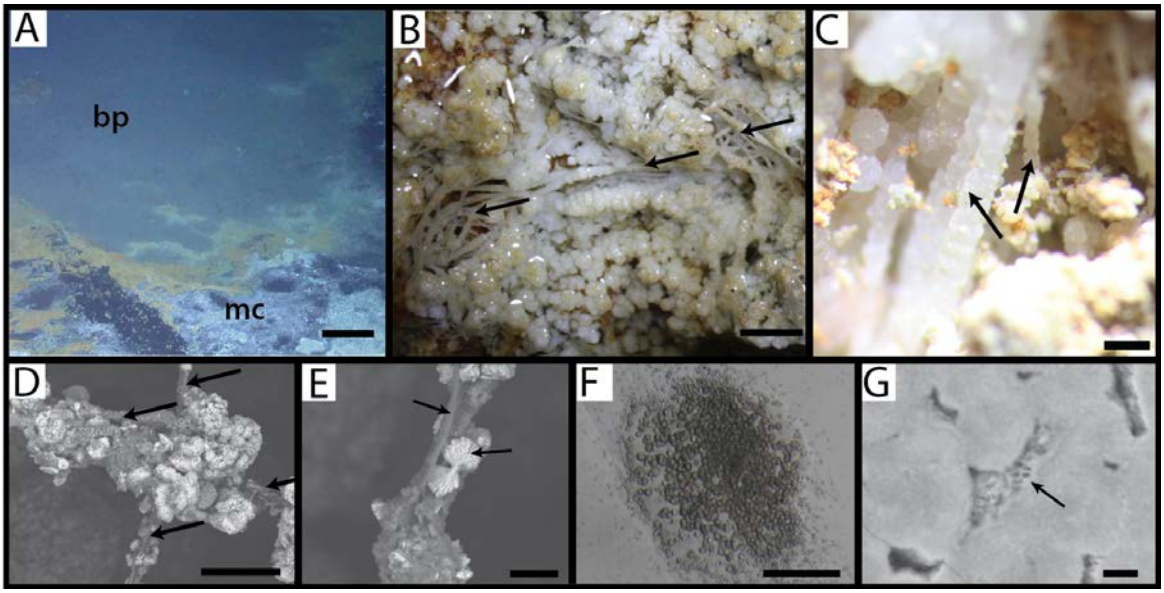

Fig. 1: A) Dead Crab Lake, a brine pool (bp) in the Gulf of Mexico, is surrounded by a complex assemblage of multi-colored mineral crusts (mc) and microbial mats containing abundant *Beggiatoa*. B) Networks of mineralized filaments (arrows) are found within barite crusts. The filament network is surrounded by barite precipitates that have a massive, non-filamentous habit. C) Detail showing barite mineral filaments that exhibit apparent septations that, if biological in origin, resemble those of *Beggiatoa* filaments. D, E) Scanning electron microscope images of bacterial filaments from Dead Crab Lake partially encrusted in barite. F) Light microscope images of barite experimentally precipitated on *Roseobacter* colony. G) Scanning electron micrographs showing morphologies of experimental barite precipitates. Arrows indicate areas of probable bacterial cells entombed within barite precipitates. Other bacterial experiments show similar encrustation of colony biomass. Scale bar in A= ~30 cm B = 1 mm, C = 100 μm, D = 40 μm, E = 10 μm; F = 100 μm, G = 3 μm.

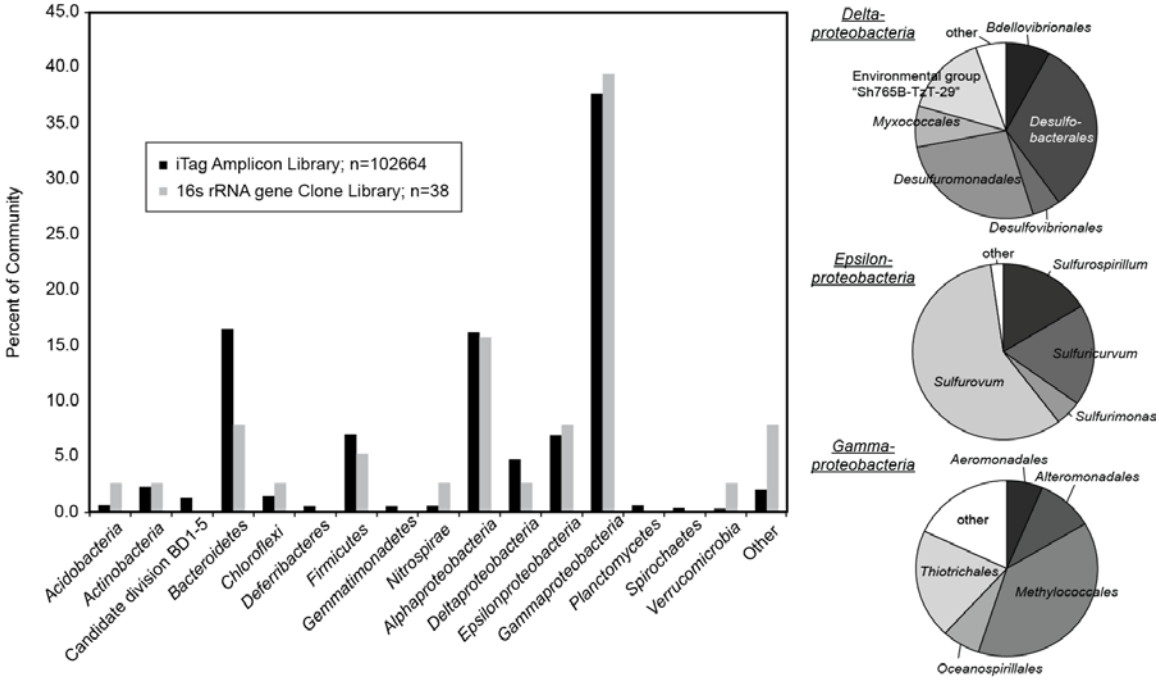

Fig. 2: Taxonomic composition of the bacterial 16S rRNA gene clone library and the 16S rRNA gene iTag amplicon library from a single filament-hosting barite crust sample. Pie charts at right summarizing a subset of the iTag results show the composition at the order level for deltaproteobacteria and gammaproteobacteria, and at the genus level for epsilonproteobacteria. Both libraries were generated from the same DNA extraction.

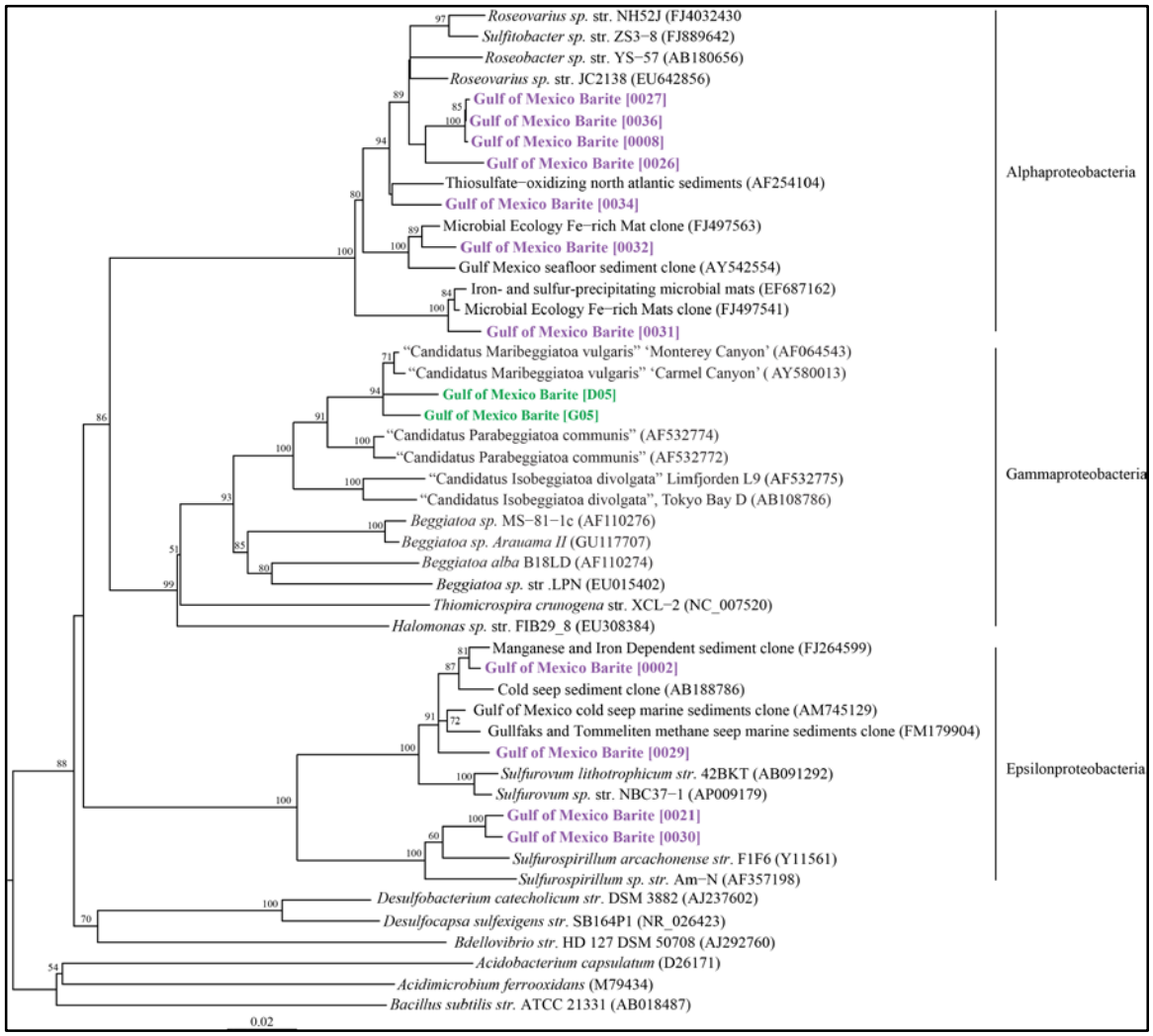

Fig. 3: Neighbor joining phylogram of 16S rRNA gene sequences from the barite crust bacterial clone library showing putative sulfide-oxidizing bacteria. Sequences generated from general bacterial primers are highlighted in purple, while sequences produced with Beggiatoaceae-specific primers are shown in green. Bootstrap values greater than 50 are shown for each node.

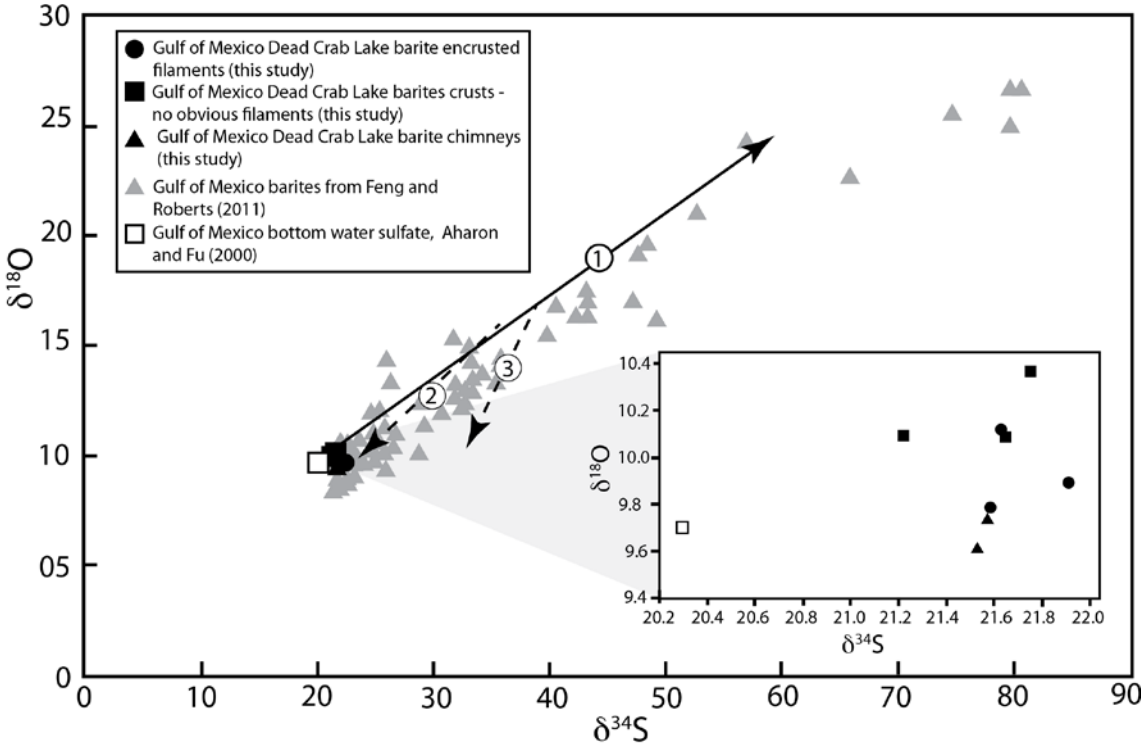

Fig. 4: $\delta^{18}O$ and $\delta^{34}S$ of sulfates and barites in the Gulf of Mexico including those reported on by Feng and Roberts (2011) (gray triangles), and those in this study that include barite mineralized filaments and surrounding barite cements, show enrichment in ^{18}O and ^{34}S. This enrichment tracks the isotopic evolution of sedimentary pore waters influenced to varying degrees by microbial sulfate reduction, the trajectory of which is shown by Arrow 1. Inset shows detail of samples from this study relative to seawater sulfate. Barites that are less enriched in ^{18}O and ^{34}S may result from lower rates of sulfate reduction, a more open system that allows for the incorporation of seawater sulfate, and/or the incorporation of sulfate produced by sulfide oxidation. Trajectories shown by Arrows 2 and 3 show varying degrees of potential oxygen isotope exchange with ambient pore water and seawater.

SUPPLEMENT

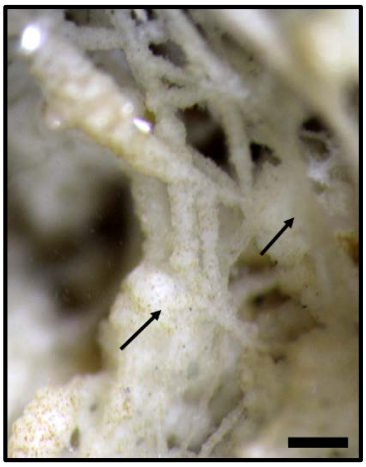

Fig. S1. Where accumulations of barite-mineralized filaments attain sufficient density, an amorphous globular barite crystal mass can result. These massive textures resemble the precipitates that make up the bulk of the barite crusts. Scale bar = 100μm.

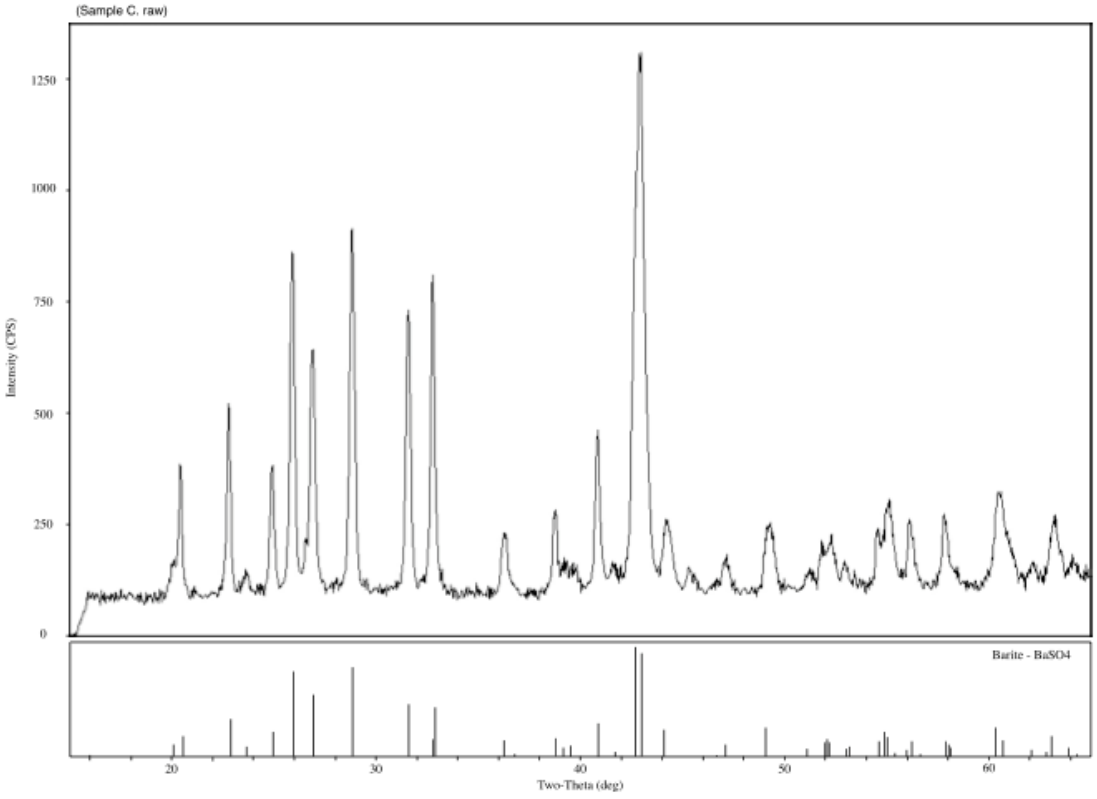

Fig. S2. X-ray diffraction diagram of precipitates found in GOM mineral crust. Typical barite ($BaSO_4$) peaks are indicated at bottom for comparison. A minor quartz (SiO_2) peak is visible at ~ 2 θ 26.5° and an unidentified peak is visible at ~ 2 θ 45°.

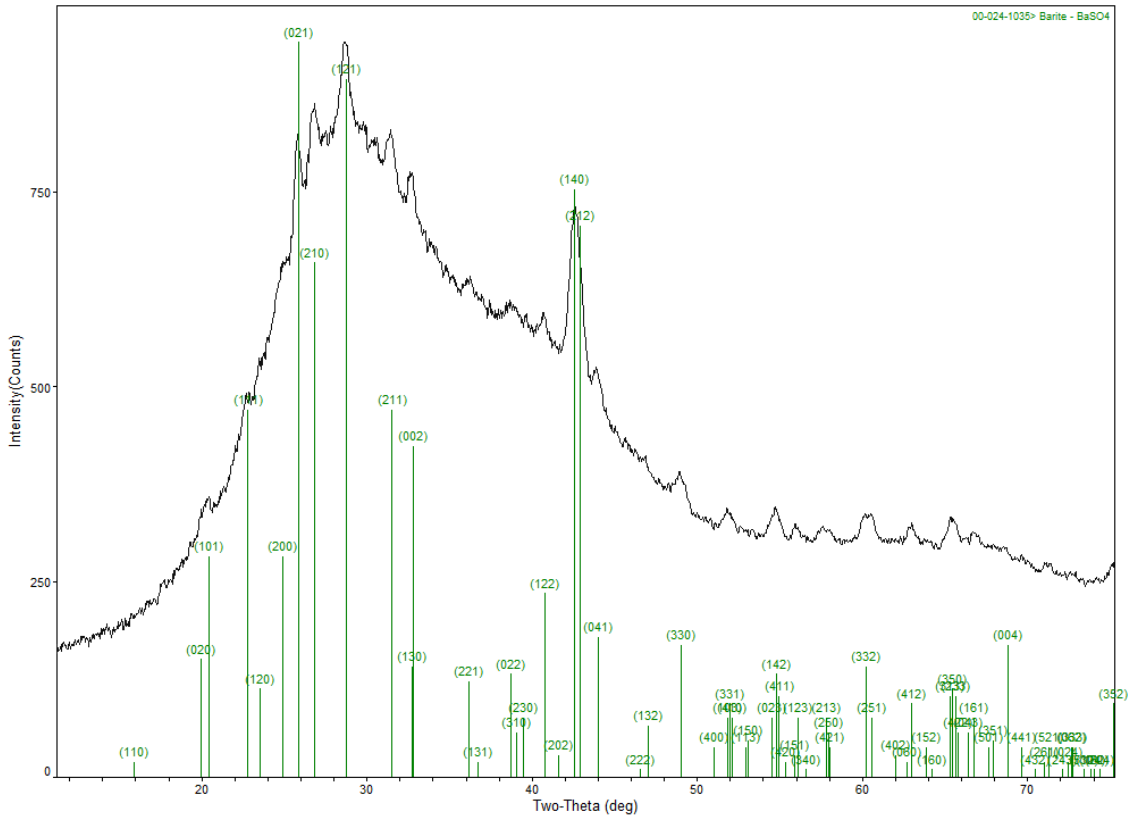

Fig. S3. Representative micro XRD diffractogram of precipitates found in laboratory precipitation experiments with *Roseobacter*. Precipitates associated with other strains were very similar to this one. Typical barite ($BaSO_4$) peaks are indicated for comparison.

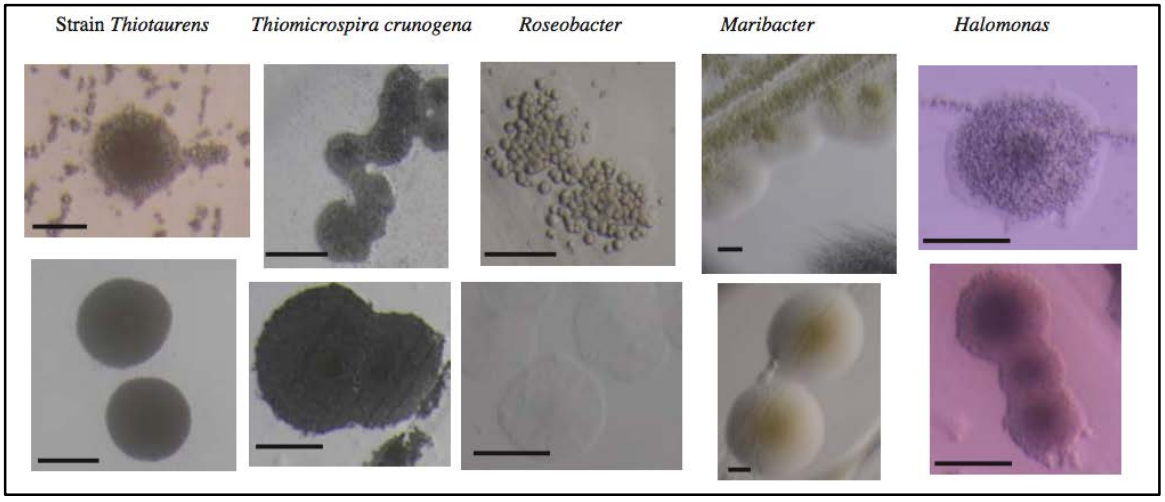

Fig. S4. Reflected light images of colonies from barite precipitation experiments. Images show precipitation results of microbial growth on media of 10 mM $Na_2S_2O_3$ with 2mM BaCl (above) and without 2mM BaCl (below). Scale bars = 100 μm.

Table S1. Primer sequences used for clone libraries, iTag and isolate screening. Illumina amplicon V3_7R contains a barcode region (shaded) used to distinguish the sample from a pooled dataset.

Primer	Sequence	Reference
EUB 27F	AGAGTTTGATCMTGGCTCAG	Lane, 1991
EUB 1492R	GGTTACCTTGTTACGACTT	Lane, 1991
EUB primer 341F	CCTACGGGAGGCAGCAG	Salman et al., 2011
VSOXBr	GGATYAATYTCCCCCAACAT	Kalanetra et al., 2005
V3_7R	caagcagaagacggcatacgagatGATCTGgtgactggagttcagacgtgtgctcttccgatctATTACCGCGGCTGCTGG	Bartram et al., 2011
V3_F modified2	aatgatacggcgaccaccgagatctacactctttccctacacgacgctcttccgatctNNNNCCTACGGGAGGCAGCAG	Bartram et al., 2011
soxB693F	ATCGGNCARGCNTTYCCNTA	Petri et al., 2001
soxB1164B	AARTTNCCNCGNCGRTA	Petri et al., 2001

Table S2.

Location	Sample type	Primary XRD mineral composition	$\delta^{34}S_{Barite}$ (‰ V-CDT)	$\delta^{18}O_{Barite}$ (‰ V-SMOW)
GC246	Chimney	Barite	21.6	9.7
GC246	Chimney	Barite	21.5	9.6
GC246	Crust	Barite	21.2	10.1
GC246	Crust	Barite	21.8	10.4
GC246	Crust	Barite	21.6	10.1
GC246	Filaments	Barite	21.9	9.9
GC246	Filaments	Barite	21.6	10.1
GC246	Filaments	Barite	21.6	9.8

REFERENCES

Addy SK, Behrens EW (1980) Time of accumulation of hypersaline anoxic brine in Orca basin (Gulf of Mexico). *Marine Geology,* **37**, 241-252.

Aharon P, Fu B (2000) Microbial sulfate reduction rates and sulfur and oxygen isotope fractionations at oil and gas seeps in deepwater Gulf of Mexico. *Geochimica et Cosmochimica Acta,* **64**, 233-246.

Aloisi G, Wallmann K, Bollwerk SM, Derkachev A, Bohrmann G, Suess E (2004) The effect of dissolved barium on biogeochemical processes at cold seeps. *Geochimica et Cosmochimica Acta,* **68**, 1735-1748.

Aquilina L, Dia AN, Boulègue J, Bourgois J, Fouillac AM (1997) Massive barite deposits in the convergent margin off Peru: Implications for fluid circulation within subduction zones. *Geochimica et Cosmochimica Acta,* **61**, 1233-1245.

Arenas C, Gutierrex F, Osacar C, Sancho C (2000) Sedimentology and geochemistry of fluvio–lacustrine tufa deposits controlled by evaporite solution subsidence in the central Ebro Depression, NE Spain. *Sedimentology,* **47**, 883–909.

Aronesty E (2011) ea-utils: Command-line tools for processing biological sequencing data. In: *Expression Analysis,* Durham, NC.

Bailey JV, Corsetti FA, Greene SE, Crosby CH, Liu P, Orphan VJ (2013) Filamentous sulfur bacteria preserved in modern and ancient phosphatic sediments: implications for the role of oxygen and bacteria in phosphogenesis. *Geobiology*, **11**, 397-405.

Barbieri R, Cavalazzi B (2005) Microbial fabrics from Neogene cold seep carbonates, Northern Apeninne, Italy. *Palaeogeography Palaeoclimatology Palaeoecology*, **227**, 143-155.

Bartram AK, Lynch MD, Stearns JC, Moreno-Hagelsieb G, Neufeld JD (2011) Generation of multimillion-sequence 16S rRNA gene libraries from complex microbial communities by assembling paired-end Illumina reads. *Applied and Environmental Microbiology*, **77**, 3846-3852.

Bertram MA, James PC (1997) Morphological and compositional evidence for biotic precipitation of marine barite. *Journal of Marine Research*, **55**, 577-593.

Bishop JKB (1988a) The barite-opal-organic carbon association in oceanic particulate matter. *Nature*, **311**, 341–343.

Blankenberg D, Kuster GV, Coraor N, Ananda G, Lazarus R, Mangan M, Nekrutenko A, Taylor J (2010) Galaxy: A Web Based Genome Analysis Tool for Experimentalists. *Current protocols in molecular biology*, 19.10. 11-19.10. 21.

Boetius A, Ravenschlag K, Schubert CJ, Rickert D, Widdel F, Gieseke A, Amann R, Jorgensen BB, Witte U, Pfannkuche O (2000) A marine microbial consortium apparently mediating anaerobic oxidation of methane. *Nature*, **407**, 623-626.

Bojanowski MJ (2007) Oligocene cold-seep carbonates from the Carpathians and their inferred relation to gas hydrates. *Facies*, **53**, 347-360.

Bonny SM, Jones B (2007a) Barite ($BaSO_4$) biomineralization at Flybye Springs, a cold sulphur spring system in Canada's Northwest Territories. *Canadian Journal of Earth Sciences*, **44**, 835-856.

Bonny SM, Jones B (2007b) Diatom-mediated barite precipitation in microbial mats calcifying at Stinking Springs, a warm sulphur spring system in Northwestern Utah, USA. *Sedimentary Geology*, **194**, 223-244.

Bonny SM, Jones B (2008a) Controls on the precipitation of barite ($BaSO_4$) crystals in calcite travertine at Twitya Spring, a warm sulphur spring in Canada's Northwest Territories. *Sedimentary Geology*, **203**, 36-53.

Bonny SM, Jones B (2008b) Experimental precipitation of barite (BaSO4) among streamers of sulfur-oxidizing bacteria. *Journal of Sedimentary Research*, **78**, 357-365.

Brabec MY, Lyons TW, Mandernack KW (2012) Oxygen and sulfur isotope fractionation during sulfide oxidation by anoxygenic phototrophic bacteria. *Geochimica et Cosmochimica Acta*, **83**, 234-251.

Bradley AS, Leavitt WD, Johnston DT (2011) Revisiting the dissimilatory sulfate reduction pathway. *Geobiology*, **9**, 446-457.

Bromberg C, Cash H, Curtis P, Goebel III C, Irwin L, Singer J, Van Hoewyk D, Winkelplek J (1995) Sequencher. Gene Codes Corporation. *Ann Arbor, Michigan*.

Brunner B, Bernasconi SM, Kleikemper J, Schroth MH (2005) A model for oxygen and sulfur isotope fractionation in sulfate during bacterial sulfate reduction processes. *Geochimica et Cosmochimica Acta*, **69**, 4773-4785.

Buchan A, Gonzalez JM, Moran MA (2005) Overview of the marine Roseobacter lineage. *Applied and Environmental Microbiology*, **71**, 5665-5677.

Campbell BJ, Engel AS, Porter ML, Takai K (2006) The versatile epsilonproteobacteria: key players in sulphidic habitats. *Nature Reviews Microbiology*, **4**, 458-468.

Castellini, D. G., et al. (2006). Barium cycling in shallow sediment above active mud volcanoes in the Gulf of Mexico. *Chemical Geology*, **226**, 1-30.

Cavagna S, Clari P, Martire L (1999) The role of bacteria in the formation of cold seep carbonates: geological evidence from Monferrato (Tertiary, NW Italy). *Sedimentary Geology*, **126**, 253-270.

Chow TJ, Goldberg ED (1960) On the marine geochemistry of barium. *Geochimica et Cosmochimica Acta*, **20**, 192-198.

Church TM, Wolgemuth K (1972) Marine barite saturation. *Earth and Planetary Science Letters*, **15**, 35-44.

Contreras S, Meister P, Liu B, Prieto-Mollar X, Hinrichs KU, Khalili A, Ferdelman TG, Kuypers MM, Jorgensen BB (2013) Cyclic 100-ka (glacial-interglacial) migration of subseafloor redox zonation on the Peruvian shelf. *Proceedings of the National Acadeny of Sciiences U S A*, **110**, 18098-18103.

Daffonchio D, Borin S, Brusa T, Brusetti L, Van Der Wielen PWJJ, Bolhuis H, Yakimov MM, D'auria G, Giuliano L, Marty D, Tamburini C, Mcgenity TJ, Hallsworth JE, Sass AM, Timmis KN, Tselepides A, De Lange GJ, Hübner A, Thomson J, Varnavas SP, Gasparoni F, Gerber HW, Malinverno E, Corselli C (2006) Stratified prokaryote network in the oxic–anoxic transition of a deep-sea halocline. *Nature*, **440**, 203-207.

Dehairs F, Chesselet R, Jedwab J (1980) Discrete suspended particles of barite and the barium cycle in the open ocean. *Earth and Planetary Science Letters*, **49**, 528-550.

Dehairs F, Stroobants N, Goeyens L (1991) Suspended barite as a tracer of biological activity in the Southern Ocean. *Marine Chemistry*, **35**, 399-410.

Desantis TZ, Hugenholtz P, Larsen N, Rojas M, Brodie EL, Keller K, Huber T, Dalevi D, Hu P, Andersen GL (2006) Greengenes, a chimera-checked 16S rRNA gene database and workbench compatible with ARB. *Applied and Environmental Microbiology*, **72**, 5069-5072.

Deusner C, Holler T, Arnold GL, Bernasconi SM, Formolo MJ, Brunner B (2014) Sulfur and oxygen isotope fractionation during sulfate reduction coupled to anaerobic oxidation of methane is dependent on methane concentration. *Earth and Planetary Science Letters*, **399**, 61-73.

Dymond J, Suess E, Lyle M (1992) Barium in deep sea sediments: A geochemical proxy for paleoproductivity. *Paleoceanography*, **163**, 181.

Eder W, Ludwig W, Huber R (1999) Novel 16S rRNA gene sequences retrieved from highly saline brine sediments of Kebrit Deep, Red Sea. *Archives of Microbiology*, **172**, 213-218.

Edgar RC, Haas BJ, Clemente JC, Quince C, Knight R (2011) UCHIME improves sensitivity and speed of chimera detection. *Bioinformatics*, **27**, 2194-2200.

Eickmann B, Thorseth IH, Peters M, Strauss H, Bröcker M, Pedersen RB (2014) Barite in hydrothermal environments as a recorder of subseafloor processes: a multiple-isotope study from the Loki's Castle vent field. *Geobiology*, **12**, 308-321.

Feng D, Roberts HH (2011) Geochemical characteristics of the barite deposits at cold seeps from the northern Gulf of Mexico continental slope. *Earth and Planetary Science Letters*, **309**, 89-99.

Flood, B, Bailey, J, Jones, D (2015) *Sedimenticola thiotaurini* sp. nov., a sulfide-oxidizing bacterium isolated from saltmarsh sediments, emended description of the genus *Sedimenticola* and holotype strain *Sedimenticola selenatireducens*. *International Journal of Systematic and Evolutionary Microbiology. doi: 10.1099/ijs.0.000295*

Fritz P, Basharmal GM, Drimmie RJ, Ibsen J, Qureshi RM (1989) Oxygen isotope exchange between sulphate and water during bacterial reduction of sulphate. *Chemical Geology*, **79**, 9-105.

Fry B, Cox J, Gest H, Hayes JM (1986) Discrimination between ^{34}S and ^{32}S during bacterial metabolism of inorganic sulfur compounds. *Journal of Bacteriology*, **165**, 328-330.

Fu, B, Aharon, P, Byerly, G, Roberts, H (1994) Barite chimneys on the Gulf of Mexico slope: initial report on their petrography and geochemistry. *Geo-Marine Letters*, **14**, 81–87.

Ganeshram RS, Francois R, Commeau J, Brown-Leger SL (2003) An experimental investigation of barite formation in seawater. *Geochimica et Cosmochimica Acta*, **67**, 2599–2605.

Gartman A, Yücel M, Madison A, Chu D, Ma S, Janzen C, Becker E, Beinart R, Girguis P, Luther G, III (2011) Sulfide oxidation across diffuse flow zones of hydrothermal vents. *Aquatic Geochemistry*, **17**, 583-601.

Giardine B, Riemer C, Hardison RC, Burhans R, Elnitski L, Shah P, Zhang Y, Blankenberg D, Albert I, Taylor J (2005) Galaxy: a platform for interactive large-scale genome analysis. *Genome Research*, **15**, 1451-1455.

Gingele F, Dahmke A (1994) Discrete barite particles and barium as a tracer of paleoproductivity in South Atlantic sediments *Paleoceanography*, **9**, 151–168.

Goldberg ED, Arrhenius G (1958) Chemistry of pelagic sediments. *Geochimica et Cosmochimica Acta*, **13**, 153–212.

Goldberg ED, Somayajulu BLK, Gallway J, Kaplan IR, Faure G (1969) Differences between barites of marine and continental origins *Geochimica et Cosmochimica Acta*, **33**, 287-289.

Gonzalez-Muñoz M, Martinez-Ruiz F, Morcillo F, Martin-Ramos J, Paytan A (2012) Precipitation of barite by marine bacteria: A possible mechanism for marine barite formation. *Geology*, **40**, 675-678.

Gonzalez-Munoz MT, Fernandez-Luque, B., Martínez-Ruiz, F., Chekroun, K.B., Arias, J.M., Rodríguez-Gallego, M., Martínez-Canamero, M., Linares, C., Paytan, A., (2003) Precipitation of barite by *Myxococcus xanthus*: possible implications for the biogeochemical cycle of barium. *Applied and Environmental Microbiology*, **69**, 5722-5725.

Greinert J, Bollwerk SM, Derkachev A, Bohrmann G, Suess E (2002) Massive barite deposits and carbonate mineralization in the Derugin Basin, Sea of Okhotsk: precipitation processes at cold seep sites. *Earth and Planetary Science Letters*, **203**, 165-180.

878 Griffith EM, Paytan A (2012) Barite in the ocean- occurrence, geochemistry and
879 palaeoceanographic applications. *Sedimentology*, doi: 10.1111/j.1365-
880 3091.2012.01327.x.
881 Habicht KS, Gade M, Thamdrup B, Berg P, Canfield DE (2002) Calibration of sulfate
882 levels in the Archean ocean. *Science,* **298**, 2372-2374.
883 Hanor JS (2000) Barite–celestine geochemistry and environments of formation. *Reviews*
884 *in Mineralogy and Geochemistry*, **40**, 193–275.
885 Jannasch HW, Wirsen CO, Nelson DC, Robertson LA (1985) *Thiomicrospira crunogena*
886 sp. nov., a colorless, sulfur-oxidizing bacterium from a deep-sea hydrothermal
887 vent. *International Journal of Systematic Bactreiology*, **35**, 422-424.
888 Jones, D.S.*, Flood, B.E. *, **Bailey, J.V.** (2015) Metatranscriptomic analysis of
889 diminutive *Thiomargarita*-like bacteria ("*Candidatus* Thiopilula spp.") from
890 abyssal cold seeps of the Barbados Accretionary Prism. *Applied and*
891 *Environmental Microbiology. **81**:3142–3156*
892 Joye SB, Boetius A, Orcutt BN, Montoya JP, Schulz HN, Erickson MJ, Lugo SK (2004)
893 The anaerobic oxidation of methane and sulfate reduction in sediments from Gulf
894 of Mexico cold seeps. *Chemical Geology*, **205**, 219-238.
895 Joye SB, Macdonald, I.R., Montoya, J.P., Peccini, M. (2005) Geophysical and
896 geochemical signatures of Gulf of Mexico seafloor brines. *Biogeosciences,* **2**,
897 295-309.
898 Kalanetra KM, Joye SB, Sunseri NR, Nelson DC (2005) Novel vacuolate sulfur bacteria
899 from the Gulf of Mexico reproduce by reductive division in three dimensions.
900 *Environmental Microbiology,* **7**, 1451-1460.
901 Kappler U, Dahl C (2001) Enzymology and molecular biology of prokaryotic sulfite
902 oxidation. *FEMS Microbiology Letters,* **203**, 1-9.
903 Kitaura T, Doke S, Azuma I, Imaida M, Miyano K, Harada K, Yabuuchi E (1983) Halo
904 production by sulfatase activity of *V. vulnificus* and *V. cholerae* O1 on a new
905 selective sodium dodecyl sulfate-containing agar medium: A screening marker in
906 environmental surveillance. *FEMS Microbiology Letters*, **17**, 205-209.
907 Lane DJ (1991) 16S/23S rRNA sequencing. In: *Nucleic acid techniques in bacterial*
908 *systematics* (ed Goodfellow SaM). Academic Press, Chichester, England, pp.
909 115–175.
910 Leavitt WD, Halevy I, Bradley AS, Johnston DT (2013) Influence of sulfate reduction
911 rates on the Phanerozoic sulfur isotope record. *Proceedings of the National*
912 *Academy of Sciences,* **110**, 11244-11249.
913 Macdonald IR, Reilly JF, Guinasso NL, Brooks JM, Carney RS, Bryant WA, Bright TJ
914 (1990) Chemosynthetic mussels at a brine-filled pockmark in the northern Gulf of
915 Mexico. *Science,* **248**, 1096-1099.
916 Mason, O.U. §, Case, D.H.§, Naehr, T.H., Lee, R.W., Thomas, R.B., Bailey, J.V., Orphan,
917 V.J., (2015) Comparison of archaeal and bacterial diversity in methane seep
918 carbonate nodules and host sediments, Eel River Basin and Hydrate Ridge, USA.
919 *Microbial Ecology. DOI 10.1007/s00248-015-0615-6.*
920 Martin MW (2011) Cutadapt removes adapter sequences from high-throughput
921 sequencing reads. *EMBnet Journal* **17**, 10-12.
922 Masella AP, Bartram AK, Truszkowski JM, Brown DG, Neufeld JD (2012) PANDAseq:
923 paired-end assembler for Illumina sequences. *BMC Bioinformatics,* **13**, 31.

924 Meyer B, Imhoff JF, Kuever J (2007) Molecular analysis of the distribution and
925 phylogeny of the *soxB* gene among sulfur-oxidizing bacteria—evolution of the
926 Sox sulfur oxidation enzyme system. *Environmental Microbiology,* **9**, 2957–2977.
927 Michel G, Nyval-Collen P, Barbeyron T, Czjzek M, Helbert W (2006) Bioconversion of
928 red seaweed galactans: a focus on bacterial agarases and carrageenases. *Applied*
929 *Microbiology and Biotechnology,* **71**, 23-33.
930 Milucka J, Ferdelman TG, Polerecky L, Franzke D, Wegener G, Schmid M, Lieberwirth
931 I, Wagner M, Widdel F, Kuypers MM (2012) Zero-valent sulphur is a key
932 intermediate in marine methane oxidation. *Nature,* **7425**, 541-546.
933 Monnin C, Jeandel C, Cattaldo T, Dehairs F (1999) The marine barite saturation state of
934 the world's oceans. *Marine Chemistry,* **65**, 253-261.
935 Mukhopadhyaya PN, Deb C, Lahiri C, Roy P (2000) A soxA gene, encoding a diheme
936 cytochrome c, and a sox locus, essential for sulfur oxidation in a new sulfur
937 lithotrophic bacterium. *Journal of Bacteriology,* **182**, 4278–4287.
938 Mußmann M, Schulz HN, Strotmann B, Kjær T, Nielsen LP, Rosselló-Mora RA, Amann
939 RI, Jørgensen BB (2003) Phylogeny and distribution of nitrate-storing *Beggiatoa*
940 spp. in coastal marine sediments. *Environmental Microbiology,* **5**, 523-533.
941 Orcutt B, Boetius A, Elvert M, Samarkin V, Joye SB (2005) Molecular biogeochemistry
942 of sulfate reduction, methanogenesis and the anaerobic oxidation of methane at
943 Gulf of Mexico cold seeps. *Geochimica et Cosmochimica Acta,* **69**, 4267-4281.
944 Orphan VJ, House CH, Hinrichs KU, Mckeegan KD, Delong EF (2001) Methane-
945 consuming archaea revealed by directly coupled isotopic and phylogenetic
946 analysis. *Science,* **293**, 484-487.
947 Paytan A, Kastner M, Campbell D, Thiemens MH (1998) Sulfur isotopic composition of
948 Cenozoic seawater sulfate. *Science,* **282**, 1459-1462.
949 Paytan A, Kastner M, Chavez FP (1996) Glacial to interglacial fluctuations in
950 productivity in the equatorial Pacific as indicated by marine barite. *Science,* **274**,
951 1355–1357.
952 Paytan A, Kastner M, Martin EE, Macdougall JD, Herbert T (1993) Marine barite as a
953 monitor of seawater strontium isotope composition *Nature,* **366**, 445–449.
954 Peckmann J, Thiel V, Reitner J, Taviani M, Aharon P, Michaelis W (2004) A microbial
955 mat of a large sulfur bacterium preserved in a Miocene methane-seep limestone
956 *Geomicrobiology Journal*, **21**, 247-255.
957 Petri R, Podgorsek L, Imhoff JF (2001) Phylogeny and distribution of the *soxB* gene
958 among thiosulfate-oxidizing bacteria. *FEMS Microbiology Letters,* **197**, 171-178.
959 Podgorsek L, Imhoff JF (1999) Tetrathionate production by sulfur oxidizing bacteria and
960 the role of tetrathionate in the sulfur cycle of Baltic Sea sediments. *Aquatic*
961 *Microbial Ecology,* **17**, 255–265.
962 Quast C, Pruesse E, Yilmaz P, Gerken J, Schweer T, Yarza P, Peplies J, Gloeckner FO
963 (2013) The SILVA ribosomal RNA gene database project: improved data
964 processing and web-based tools. *Nucleic Acids Research,* **41** D1: D590-D596.
965 Rasmussen B (2000) Filamentous microfossils in a 3,235-million-year-old volcanogenic
966 massive sulphide deposit. *Nature,* **405**, 676-679.
967 Riedinger, N., Kasten, S., Gröger, J., Franke, C., Pfeifer, K. (2006) Active and buried
968 authigenic barite fronts in sediments from the Eastern Cape Basin. *Earth and*
969 *Planetary Science Letters,* **241**, 876-887.

970 Ritger S, Carson B, Suess E (1987) Methane-derived authigenic carbonates formed by
971 subduction-induced pore-water expulsion along the Oregon/Washington margin.
972 *Geological Society of America Bulletin*, **98**, 147-156.
973 Roberts HH, Feng D, Joye SB (2010) Cold seep carbonates of the middle and lower
974 continental slope, northern Gulf of Mexico. *Deep Sea Research,* **57**, 2040–2054.
975 Rushdi AI, Mcmanus J, Collier RW (2000) Marine barite and celestite saturation in
976 seawater. *Marine Chemistry*, **69**, 19-31.
977 Salman V, Amann R, Girnth A-C, Polerecky L, Bailey JV, Høgslund S, Jessen G, Pantoja
978 S, Schulz-Vogt HN (2011) A single-cell sequencing approach to the classification
979 of large, vacuolated sulfur bacteria. *Systematic and Applied Microbiology*, **34**,
980 243-259.
981 Salman V, Amann R, Shub DA, Schulz-Vogt HN. (2012) Multiple self-splicing introns in
982 the 16S rRNA genes of giant sulfur bacteria. *Proc. Nat. Acad. Sci. U.S.A.* **109**,
983 4203- 4208.
984 Sanz-Montero ME, Rodríguez-Aranda JP, García Del Cura MA (2009) Bioinduced
985 precipitation of barite and celestite in dolomite microbialites. Examples from
986 Miocene lacustrine sequences in the Madrid and Duero Basins, Spain.
987 *Sedimentary Geology*, **222**, 138-148.
988 Schloss PD, Westcott SL, Ryabin T, Hall JR, Hartmann M, Hollister EB, Lesniewski RA,
989 Oakley BB, Parks DH, Robinson CJ, Sahl JW, Stres B, Thallinger GG, Van Horn
990 DJ, Weber CF (2009) Introducing mothur: Open-Source, Platform-Independent,
991 Community-Supported Software for Describing and Comparing Microbial
992 Communities. *Appl. Environ. Microbiol.*, **75**, 7537-7541.
993 Scott KM, Sievert SM, Abril FN, Ball LA, Barrett CJ, Blake RA, Boller AJ, Chain PS,
994 Clark JA, Davis CR, Detter C, Do K, Dobrinski KP, Faza BI, Fitzpatrick KA,
995 Freyermuth SK, Harmer TL, Hauser LJ, Hugler M, Kerfeld CA, Kong WW, Land
996 M, Lapidus A, Larimer FW, Longo DL, Lucas S, Malfatti S, Massey SE, Martin
997 DD, Mccuddin Z, Meyer F, Moore JL, Ocampo LH, Paul JH, Paulsen IT, Reep
998 DK, Ren Q, Ross RL, Sato PY, Thomas P, Tinkham LE, Zeruth GT (2006) The
999 genome of the deep-sea vent chemolithoautotroph *Thiomicrospira crunogena*.
1000 *PLoS Biology*, **4**, 1-17.
1001 Sekar R, Mills DK, Remily ER, Voss JD, Richardson LL. **(**2006) Microbial
1002 communities in the surface mucopolysaccharide layer and the black band
1003 microbial mat of black band-diseased *Siderastrea siderea*. *Appl. Environ.*
1004 *Microbiol.* **72**, 5963-5973.
1005 Senko JM, Campbell BS, Henriksen JR, Elshahed MS, Dewers TA, Krumholz LR (2004)
1006 Barite deposition resulting from phototrophic sulfide-oxidizing bacterial activity.
1007 *Geochimica et Cosmochimica Acta*, **68**, 773-780.
1008 Shen Y, Buick R, Canfield DE (2001) Isotopic evidence for microbial sulphate reduction
1009 in the early Archaean era. *Nature*, **410**, 77-81.
1010 Sim MS, Bosak T, Ono S (2011) Large sulfur isotope fractionation does not require
1011 disproportionation. *Science*, **333**, 74-77.
1012 Sorokin DY, Teske A, Robertson LA, Kuenen JG (1999) Anaerobic oxidation of
1013 thiosulfate to tetrathionate by obligately heterotrophic bacteria, belonging to the
1014 Pseudomonas stutzeri group. *FEMS Microbiology Ecology*, **30**, 113–123.

Spirakis CS (1991) The possible role of thiosulfate in the precipitation of 34S-rich barite in some Mississippi Valley-type deposits. *Mineralium Deposita,* **26**, 60–65.

Stroobants N, Dehairs F, Goeyens L, Vanderheijden N, Van Grieken R (1991) Barite formation in the Southern Ocean water column. *Marine Chemistry*, **35**, 411-421.

Swofford D (1999) Phylogenetic analysis using parsimony (and other methods) PAUP* 4.0. *Sinauer, Sunderland*.

Teske A, Brinkhoff T, Muyzer G, Moser D, Rethmeier J, Jannasch HW (2000) Diversity of thiosulfate-oxidizing bacteria from marine sediments and hydrothermal vents. *Applied and Environmental Microbiology*, **66**, 3125-3133.

Torres ME, Bohrmann G, Dube TE, Poole FG (2003) Formation of modern and Paleozoic stratiform barite at cold methane seeps on continental margins. *Geology*, **31**, 897-900.

Torres ME, Bohrmann G, Suess E (1996) Authigenic barites and fluxes of barium associated with fluid seeps in the Peru subduction zone. *Earth and Planetary Science Letters*, **144**, 469-481.

Van Der Wielen PWJJ, Bolhuis H, Borin S, Daffonchio D, Corselli C, Giuliano L, D'auria G, De Lange GJ, Huebner A, Varnavas SP, Thomson J, Tamburini C, Marty D, Mcgenity TJ, Timmis KN, Party BS (2005) The Enigma of Prokaryotic Life in Deep Hypersaline Anoxic Basins. *Science,* **307**, 121-123.

Wankel SD, Bradley AS, Eldridge DL, Johnston DT (2014) Determination and application of the equilibrium oxygen isotope effect between water and sulfite. *Geochimica et Cosmochimica Acta,* **125**, 694-711.

Zerkle AL, Farquhar J, Johnston DT, Cox RP, Canfield DE (2009) Fractionation of multiple sulfur isotopes during phototrophic oxidation of sulfide and elemental sulfur by a green sulfur bacterium. *Geochimica et Cosmochimica Acta,* **73**, 291-306.